Article

Climate warming increases extreme daily wildfire growth risk in California

https://doi.org/10.1038/s41586-023-06444-3

Received: 22 July 2022

Accepted: 17 July 2023

Published online: 30 August 2023

Check for updates

Patrick T. Brown[1,2,3]✉, Holt Hanley[2,4,5], Ankur Mahesh[6,7], Colorado Reed[8], Scott J. Strenfel[9], Steven J. Davis[10], Adam K. Kochanski[2,4] & Craig B. Clements[2,4]

California has experienced enhanced extreme wildfire behaviour in recent years[1–3], leading to substantial loss of life and property[4,5]. Some portion of the change in wildfire behaviour is attributable to anthropogenic climate warming, but formally quantifying this contribution is difficult because of numerous confounding factors[6,7] and because wildfires are below the grid scale of global climate models. Here we use machine learning to quantify empirical relationships between temperature (as well as the influence of temperature on aridity) and the risk of extreme daily wildfire growth (>10,000 acres) in California and find that the influence of temperature on the risk is primarily mediated through its influence on fuel moisture. We use the uncovered relationships to estimate the changes in extreme daily wildfire growth risk under anthropogenic warming by subjecting historical fires from 2003 to 2020 to differing background climatological temperatures and aridity conditions. We find that the influence of anthropogenic warming on the risk of extreme daily wildfire growth varies appreciably on a fire-by-fire and day-by-day basis, depending on whether or not climate warming pushes conditions over certain thresholds of aridity, such as 1.5 kPa of vapour-pressure deficit and 10% dead fuel moisture. So far, anthropogenic warming has enhanced the aggregate expected frequency of extreme daily wildfire growth by 25% (5–95 range of 14–36%), on average, relative to preindustrial conditions. But for some fires, there was approximately no change, and for other fires, the enhancement has been as much as 461%. When historical fires are subjected to a range of projected end-of-century conditions, the aggregate expected frequency of extreme daily wildfire growth events increases by 59% (5–95 range of 47–71%) under a low SSP1–2.6 emissions scenario compared with an increase of 172% (5–95 range of 156–188%) under a very high SSP5–8.5 emissions scenario, relative to preindustrial conditions.

Physics-based models are typically the preferred means of quantifying the contribution of increased greenhouse gas concentrations to weather and climate extremes[8]. However, high-resolution physics-based models capable of simulating fire behaviour at daily timescales and kilometre spatial scales[9] are too computationally expensive to easily incorporate into climate change studies. Many dynamic global vegetation models designed for climate change studies simulate fire characteristics[10] but they output at spatiotemporal resolutions too coarse to make inferences about the extreme daily growth of individual fires (Supplementary Information 22). These practical constraints have led much research to focus on the influence of anthropogenic forcing on conditions conducive to wildfires[11–18] calculated by global climate models (Supplementary Information 23). Studies often make use of fire-weather or fire-danger indices, which have the relationship between temperature and conduciveness to wildfires presupposed.

Here our goal is to isolate and quantify the influence of anthropogenic warming on the risk of extreme wildfire behaviour in California at the daily timescale and kilometre spatial scale. We also seek to make attribution statements at the level of individual fires. We overcome the aforementioned practical constraints of using physics-based models by using a machine learning approach[19–22].

Rather than assuming a specific statistical or functional relationship between temperature and extreme wildfire behaviour, using this approach we learn the relationship between temperature and wildfire behaviour directly from the data. Specifically, we use neural networks and random forests to learn the potentially nonlinear relationship between temperature and wildfire behaviour in ways that are highly conditional on the state of other environmental variables.

Extreme wildfire behaviour has many defining charecteristics[23], and here we focus on just one of those aspects: extremely high rates of growth in burnt areas of 10,000 acres (about two-thirds of the size

[1]Climate and Energy Team, The Breakthrough Institute, Berkeley, CA, USA. [2]Wildfire Interdisciplinary Research Center (WIRC), San José State University, San Jose, CA, USA. [3]Energy Policy and Climate Program, Johns Hopkins University, Baltimore, MD, USA. [4]Department of Meteorology and Climate Science, San José State University, San Jose, CA, USA. [5]KSBW News, Salinas, CA, USA. [6]Climate and Ecosystems Division, Lawrence Berkeley National Laboratory, Berkeley, CA, USA. [7]Earth and Planetary Science, University of California, Berkeley, Berkeley, CA, USA. [8]Electrical Engineering and Computer Sciences, University of California, Berkeley, Berkeley, CA, USA. [9]Pacific Gas and Electric Company, Oakland, CA, USA. [10]Department of Earth System Science, University of California, Irvine, Irvine, CA, USA. ✉e-mail: Patrick@thebreakthrough.org

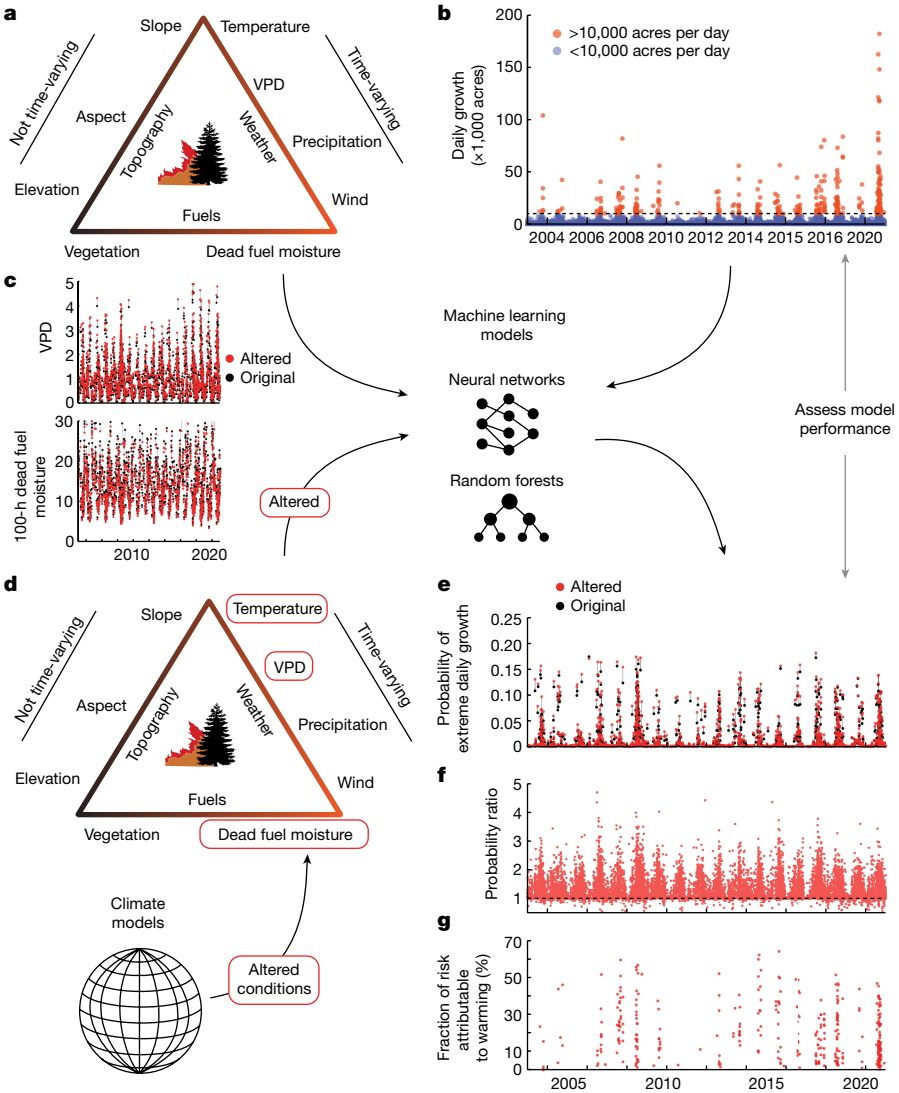

Fig. 1 | Illustration of the method. a–e, An ensemble of neural networks and random forests learn the relationships between environmental predictor variables (Supplementary Table 2; there are two predictor variables for vegetation and two for dead fuel moisture and the probability of occurrence of daily wildfire growth of more than 10,000 acres. VPD, vapour-pressure deficit; Wind, wind speed. **c–e**, The probability of occurrence of extreme growth is recalculated, incorporating shifts in background climatological temperature produced from global climate models (Supplementary Fig. 2). Temperature changes are also propagated into aridity variables that have a direct relationship with temperature (Supplementary Information equations 3–10). **e**, Predicted probability of extreme daily growth for present (red) compared with preindustrial (black) conditions with each event connected by a black line. For clarity, a random sampling of only 2,000 (out of 17,910) fire-days is shown. **f**, Probability ratios for the two probabilities shown in **e** (Supplementary Information equation 1). **g**, Fraction of the risk of extreme daily growth attributable to anthropogenic warming (Supplementary Information equation 2). All results in **e–g** are calculated outside of the training set so that predictive skill can be assessed along with the results. These are calculated using leave-3-years-out cross-validation (Supplementary Fig. 3). All results in **e–g** are averages of the top 10% of machine learning model configurations in terms of their log-loss scores (black dots in Supplementary Figs. 3a,b and 4). See Supplementary Information 1 and a video explanation of the method for further details (https://youtu.be/lHztGWzghRI).

of Manhattan) or more in a single day. We focus on this class of events because these events have been disproportionately responsible for the exponential increase in the observed annual burnt area[1,2], and they are particularly challenging from a firefighting perspective, which increases the likelihood of loss of life and property.

Our approach can be summarized in two steps. (1) We train an ensemble of machine learning models to learn the relationships between environmental conditions (predictors) and the risk of extreme daily fire growth (response), given an active fire (Fig. 1a,b and Supplementary Information 1). (2) We then alter the predictor values based on global climate model simulations of anthropogenic warming and recalculate the risk (Fig. 1c–e). Thus, we hold everything about historical conditions during fire-days constant (that is, fuel characteristics, ignitions, winds, precipitation and absolute humidity) except for the background climatological temperature. This approach, similar to the pseudo-global warming[24] or storyline approaches[8,25] of the extreme event attribution literature[26], enables us to investigate the influence of warming on risk at the granularity of individual days for historical fires. We choose to isolate the influence of temperature on the risk of extreme daily fire growth because temperature is the variable in the wildfire-behaviour triangle (Fig. 1a) that is by far the most directly related to increasing greenhouse gas concentrations and, thus, the most well-constrained in future projections. Furthermore, it has been demonstrated that interannual temperature variations are strongly associated with variations in wildfire activity, especially in forests where fires are aridity limited (as opposed to fuel limited)[12,27–29].

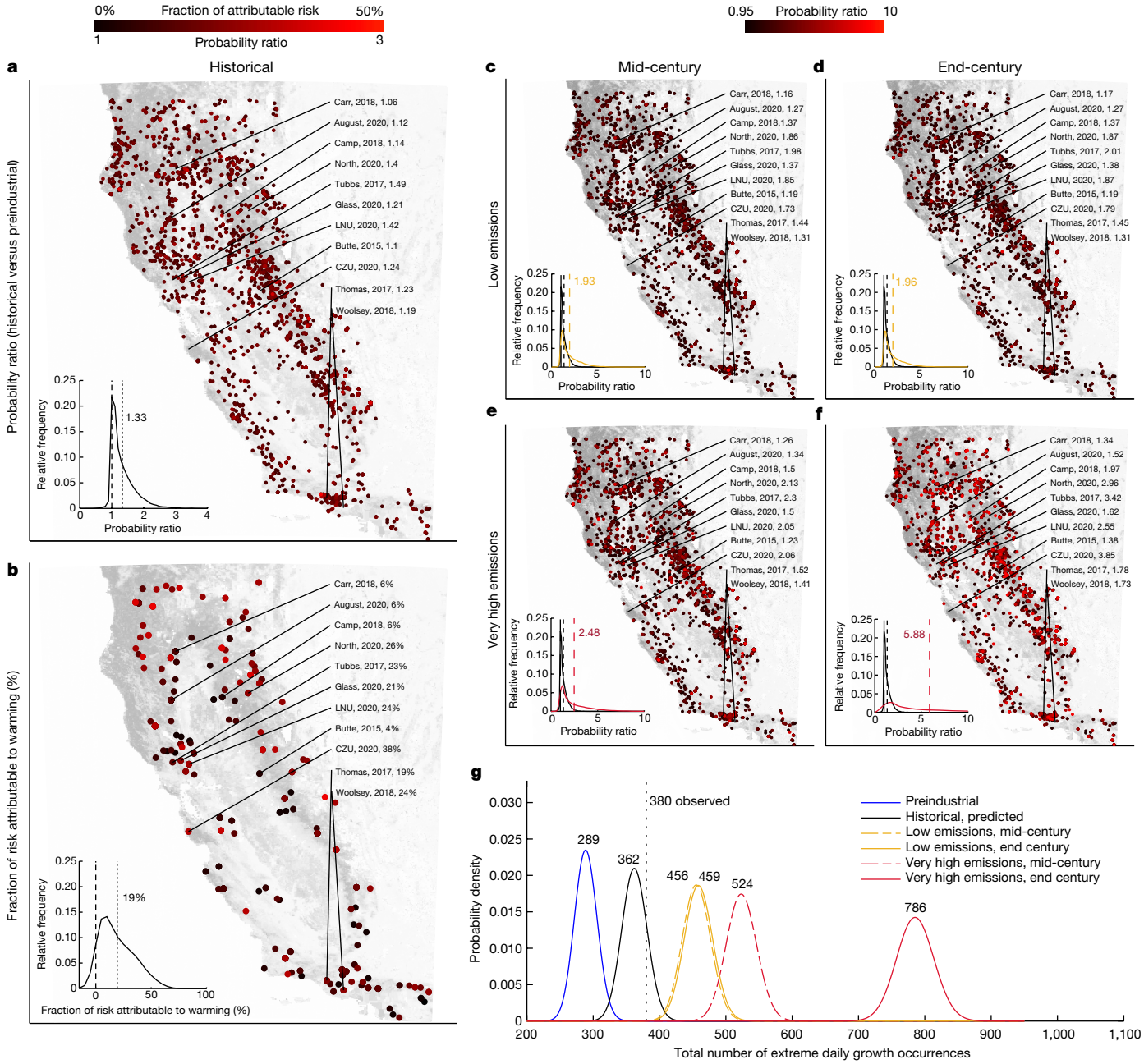

Fig. 2 | Influence of anthropogenic warming on the risk of extreme wildfire behaviour historically and in the future. a, Probability ratios for all fire-days in the present relative to preindustrial, averaged over the 10% of machine learning model configurations that performed the best on out-of-sample historical data (Supplementary Information 10–17). **b**, Same as **a** but for the fraction of risk attributable to anthropogenic warming and only those fire-days with daily growth of more than 10,000 acres considered. **a** and **b** show the same information as Fig. 1f and 1g, respectively, but the information is displayed in space rather than in time. **c**–**f**, Probability ratios for all fire-days in the dataset for mid-century (**c**,**e**) and end century (**d**,**f**) and for a low-emissions scenario (SSP1–2.6; **c**,**d**) and a very-high-emissions scenario (SSP5–8.5; **e**,**f**). Fires notable for causing large damage are highlighted (August refers to the August Complex Fire; North to the North Complex Fire; LNU to the LNU Lightning Complex fires; and CZU to the CZU Lightning Complex fires). The probability ratios for these fires are calculated as a mean daily probability of extreme growth over the lifetime of fire in the altered climate divided by the mean daily probability over the lifetime of fire in the preindustrial climate (as opposed to the mean of the daily probability ratios; Supplementary Information equations 19 and 20). Insets, kernel density estimates fit to the probability ratio distributions across all fire-days. Vertical lines in the insets are the distribution means. The historical distribution (black) is reproduced in **c**–**f** for context. **g**, Poisson distributions for the expected aggregate frequency of extreme growth days for historical fire-days under different background climatological temperatures. The values reported in this study refer to the median and 5th and 95th percentiles of these Poisson distributions where the historical and end-of-century SSP1–2.6 and SSP5–8.5 scenarios are compared with the preindustrial conditions.

It is already well established that the influence of temperature on wildfire behaviour is not primarily through temperature[30], but through the influence of temperature on aridity[12,13,31]. Thus, we also propagate changes in temperature into the three other predictor variables that have the most direct relationships with temperature (Fig. 1c). These variables are vapour-pressure deficit and the two calculated dead fuel moisture variables (100 h and 1,000 h; Supplementary Information 5).

The central results of this study compare the calculated risks under preindustrial conditions and the calculated risks under warmed

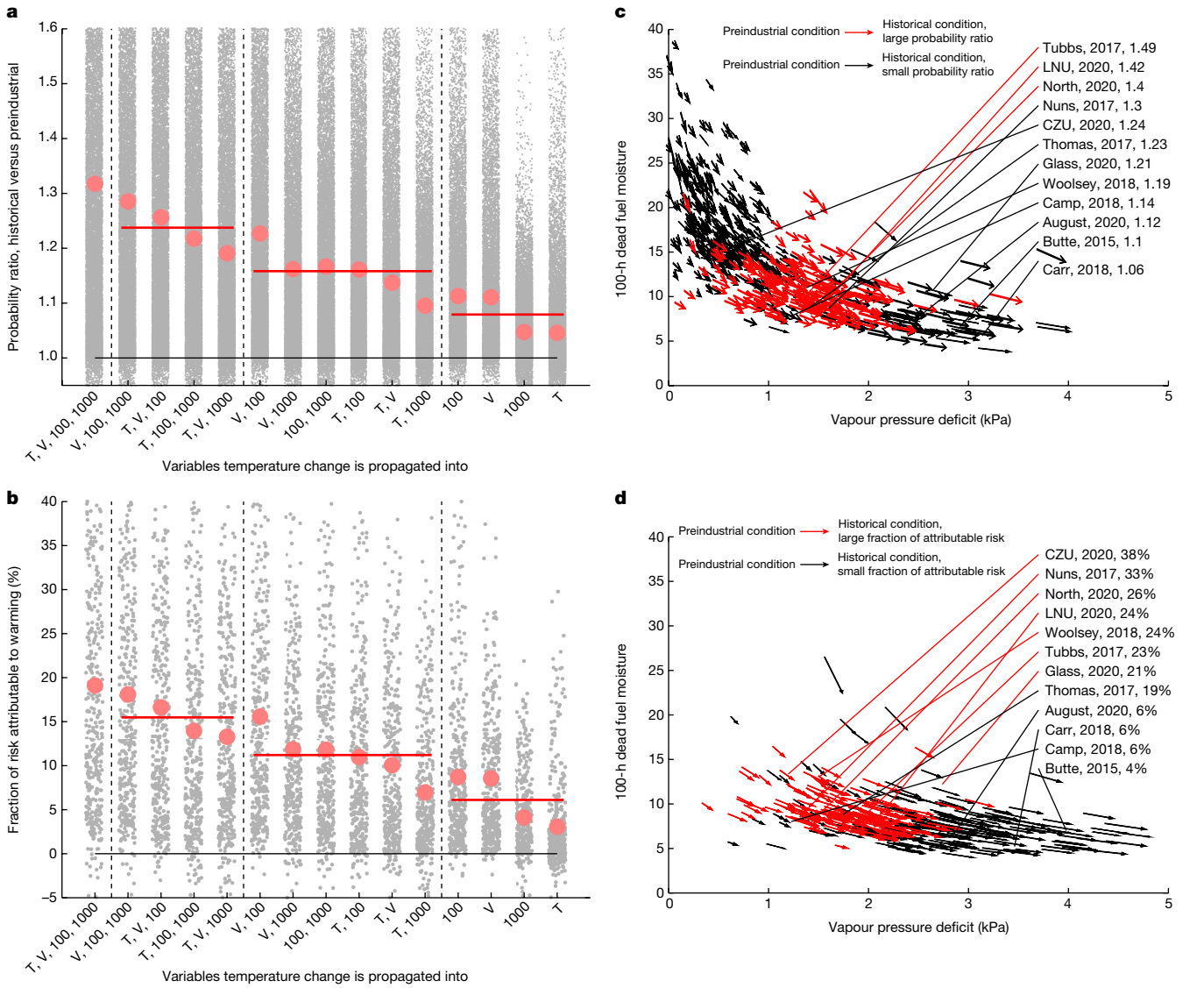

Fig. 3 | Physical conditions and mechanisms most responsible for shifts in the risk of extreme wildfire growth. a,**b**, The effect of propagating anthropogenic warming into different combinations of the four predictors most directly influenced by temperature. Each grey dot represents a fire-day, and the red circles are distribution means (the far-left column in **a** and **b** show the same distributions as the insets in Fig. 2a,b). The letters on the *x* axis show which predictors temperature change is propagated into: T = temperature, V = vapour-pressure deficit, 100 = 100-h dead fuel moisture and 1000 = 1,000-h dead fuel moisture. **c**, The shift in parameter space, from preindustrial to historical conditions, for 100-h dead fuel moisture and vapour-pressure deficit (800 fire-days were randomly selected from the dataset for clarity). **d**, Same as **c** but for the fraction of risk attributable to warming for all 380 extreme growth days. In **c** and **d**, the origin of each arrow represents the conditions of fire-days in the preindustrial climate, and the tip of each arrow represents the conditions for the historical period. Red indicates that a probability ratio (**c**) or fraction of attributable risk (**d**) is above the mean value of the distribution. Above-average probability ratios and fractions of attributable risk are centred at about 10% 100-h dead fuel moisture and at about 1.5 kPa vapour-pressure deficit, indicating that these values represent important thresholds (see also Supplementary Information Section S21). Values for fires notable for causing large damage are highlighted in which the parameter values are means over the lifetimes of fire.

conditions using the probability ratio[32] (Fig. 1f and Supplementary Information Equation 1). For historical extreme growth events, we also calculate the fraction of the risk of that event occurring that can be attributed to anthropogenic warming[33] (Fig. 1g and Supplementary Information Equation 2. See Supplementary Information 1 as well as a video description of the method (https://youtu.be/lHztGWzghRI).

Probability ratios for the historical period, relative to preindustrial, range from slightly below 1 to more than 5 but have a mean of 1.33 (Figs. 1f and 2a). For the 380 extreme daily growth events that took place from 2003 to 2020 (out of 17,910 total fire-days), the fraction of the risk attributable to anthropogenic warming was as high as 65% and had a mean of 19% (5–95 range of +16–22%) (Figs. 1g and 2b and Supplementary Fig. 3).

By mid-century, the mean probability ratio continues to increase from 1.33 and ranges from 1.93 in the SSP1–2.6 low-emissions scenario to 2.48 in the SSP5–8.5 very-high-emissions scenario (Fig. 2c,e). In the low-emissions scenario, the mean probability ratio is essentially stabilized from mid-century onwards as it increases to only 1.96 by the end of the century (Fig. 2d). By contrast, under the very-high-emissions scenario, the average probability ratio reaches 5.88 by the end of the century (Fig. 2f), indicating that future emissions have large leverage on future extreme wildfire behaviour.

The shifts in daily risk indicate that the historical period has experienced an aggregate expected increase in extreme daily growth frequency of 25% relative to preindustrial (362 versus 289, Fig. 2g). Going forward, the expected frequency of occurrence continues to increase

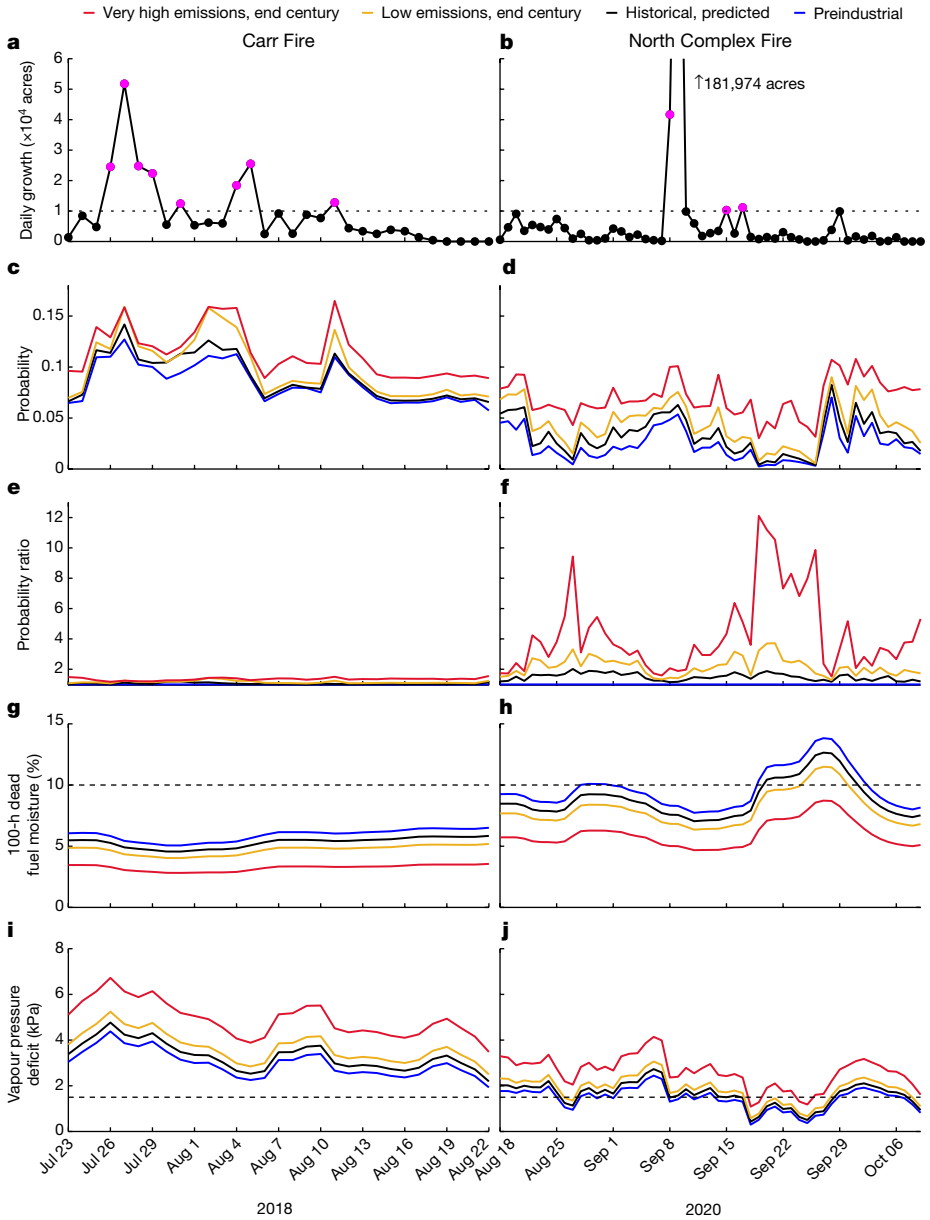

Fig. 4 | Influence of anthropogenic warming on the risk of extreme daily wildfire growth over the lifetimes of the Carr Fire and the North Complex Fire. a,b Daily fire growth, with extreme daily growth highlighted in magenta. **c**,**d**, Machine learning model calculated risk of extreme daily growth (trained on other fires) under differing levels of anthropogenic warming. **e**,**f**, Same as **c**,**d** but change in risk expressed as the probability ratio (Supplementary Information equation 1) relative to preindustrial risk. **g**,**h**, 100-h dead fuel moisture percentage. **i**,**j**, Vapour-pressure deficit (kPa). The preceding two predictor variables are highlighted here because they were found to be the most influential on probability ratios (Fig. 3a,b). The same diagrams for the other highlighted fires are shown in Supplementary Figs. 10–12.

through mid-century, but it can be stabilized at an average of +59% (459 versus 289) at the end of the century under low SSP1–2.6 emissions, compared with +90% (550 versus 289) under middle SSP2–4.5 emissions and +172% (786 versus 289) at the end of the century under very high SSP5–8.5 emissions (Fig. 2g). Stating those projections relative to what was observed over the 2003–2020 period, they are +21% (459 versus 380) at the end of the century under low SSP1–2.6 emissions, +45% (550 versus 380) under middle SSP2–4.5 emissions, and +107% (786 versus 380) at the end of the century under very high SSP5–8.5 emissions (Fig. 2g). It must be emphasized that these are idealized calculations that hold fire-days constant and isolate the influence of temperature and the direct impact of temperature on aridity. They do not incorporate potentially exacerbating factors such as changes in ignition proclivity, fire-season length or fire lifetimes, nor do they incorporate potentially mitigating factors such as enhanced fire suppression efforts or intentional management of fuels.

Figure 3a,b shows the effect of propagating temperature into all combinations of the four predictor variables with the most direct relationships with temperature (Supplementary Information 5). The highest probability ratios and fractions of attributable risk are calculated when temperature change is propagated into all three aridity predictors in addition to temperature itself (Fig. 3a,b, far-left column). When propagating into only three variables, the three aridity variables have the largest impact. When propagating into only two variables, vapour-pressure deficit and 100-h dead fuel moisture have the largest impact, and when propagating into only one variable, 100-h dead fuel

moisture has the largest impact. In all combinations, the direct effect of temperature is the least important variable, confirming that the impact of temperature is felt primarily through its effect on the atmospheric capacity for water vapour and, thus, fuel moisture[12,13,31].

We highlight several fires that were notable for causing a large amount of structural damage (labelled fires in Figs. 2, 3c,d and 4 and Supplementary Figs. 10–12). We find that the influence of anthropogenic warming on the risk of extreme daily growth varies markedly between these fires (Fig. 2). For example, the mean probability ratio over the lifetime of the North Complex Fire was 1.4 at the time of occurrence and would reach 2.96 under very high emissions at the end of the century, whereas the mean probability ratio over the lifetime of the Carr Fire was only 1.06 at the time of occurrence and would reach only 1.34 under very high emissions at the end of the century. Similarly, for the days that did see extreme growth, the fraction of risk attributable to warming was 26% for the North Complex Fire and only 6% for the Carr Fire. The influence of warming on risk varies substantially between days for the same fire (Fig. 4). For example, the probability ratios for very high emissions at the end of the century range from below 2 to more than 12 for the North Complex Fire over its lifetime (Fig. 4f).

This variation in the change in risk is not primarily because of geographic or seasonal variation in the magnitude of anthropogenic warming, which is relatively uniform (Fig. 1 and Supplementary Fig. 2). Rather, differences arise because some fire-days are very near critical aridity thresholds that have an outsized impact on the risk of extreme growth. In particular, crossing about 10% 100-h dead fuel moisture from above and/or crossing approximately 1.5 kPa vapour-pressure deficit from below (the two predictor variables most responsible for relative shifts in probability; Fig. 3a,b) greatly enhances the risk of extreme daily growth (Fig. 3c,d, red arrows). Fire-days safely on the moist side or far on the dry side of these thresholds (Fig. 3c,d, black arrows) do not experience large relative shifts in probability from anthropogenic warming and drying. Moreover, although it is often noted in this context that saturation vapour pressure increases exponentially with temperature, dead fuel moisture decreases asymptotically with temperature, indicating diminishing returns for the impact of warming on fuel moisture (anticlockwise turning of arrows as the vapour-pressure deficit increases in Fig. 3c,d).

The influences of critical thresholds and diminishing returns are seen over the lifetimes of fires as well (Fig. 4). For example, the Carr Fire occurred under very dry conditions, such that its daily mean probability of extreme growth was larger under preindustrial conditions than that of the North Complex Fire for very high emissions at the end of the century (Fig. 4c,d). Thus, even under preindustrial conditions, the Carr Fire maintained 100-h dead fuel moistures below 10% and vapour-pressure deficits above 1.5 kPa over its entire life (Fig. 4g,i, respectively), resulting in low probability ratios from anthropogenic warming (Fig. 4e). By contrast, the North Complex Fire occurred under conditions straddling the critical thresholds (that is, its growth was weather limited[34]), so anthropogenic warming had a much larger impact on its probability ratios (Fig. 3f). Correspondingly, as day-to-day weather variability moves the entire ensemble of time series away from the thresholds, probability ratios dip to local minimums (for example, 3–12 September 2020 for the North Complex Fire; Fig. 4f,h,j).

Overall, our results indicate that anthropogenic warming (and the influence of warming on aridity, holding all else constant) increases the risk of extreme daily wildfire growth in California. Our findings, however, must be interpreted narrowly as idealized calculations because temperature is only one of the dozens of important variables that influences wildfire behaviour. Nonetheless, temperature is the variable in the wildfire behaviour triangle (Fig. 1a) that is the most directly related to increasing greenhouse gas concentrations and, in our judgement, there is no expert or model consensus on the magnitude or even the direction of change of many other variables relevant to the projection of wildfire behaviour[35]. Despite this, our calculations may result in conservative estimates of changes in risk because at least several important variables that we hold constant (for example, precipitation[36], wind[11], absolute humidity[18,37], tree mortality[38], fire-season length[15,39,40] and lifetimes of fires[2]) may be changing in a way that would exacerbate the enhanced risk caused by warming rather than ameliorate it. A more comprehensive assessment of future risk would also account for changes in fuel characteristics (from intentional fuel management as well as in response to climate change), changes in fire suppression efforts and changes in ignition patterns.

Online content

Any methods, additional references, Nature Portfolio reporting summaries, source data, extended data, supplementary information, acknowledgements, peer review information; details of author contributions and competing interests; and statements of data and code availability are available at https://doi.org/10.1038/s41586-023-06444-3.

1. Coop, J. D. et al. Extreme fire spread events and area burned under recent and future climate in the western USA. *Glob. Ecol. Biogeogr.* **31**, 1949–1959 (2022).
2. Juang, C. S. et al. Rapid growth of large forest fires drives the exponential response of annual forest-fire area to aridity in the western United States. *Geophys. Res. Lett.* **49**, e2021GL097131 (2022).
3. Keeley, J. E. & Syphard, A. D. Large California wildfires: 2020 fires in historical context. *Fire Ecol.* **17**, 22 (2021).
4. Wang, D. et al. Economic footprint of California wildfires in 2018. *Nat. Sustain.* **4**, 252–260 (2021).
5. Bowman, D. M. J. S. et al. Human exposure and sensitivity to globally extreme wildfire events. *Nat. Ecol. Evol.* **1**, 0058 (2017).
6. Starrs, C. F., Butsic, V., Stephens, C. & Stewart, W. The impact of land ownership, firefighting, and reserve status on fire probability in California. *Environ. Res. Lett.* **13**, 034025 (2018).
7. Bowman, D. M. J. S. et al. Vegetation fires in the Anthropocene. *Nat. Rev. Earth Environ.* **1**, 500–515 (2020).
8. Seneviratne, S. I. et al. in *Climate Change 2021: The Physical Science Basis. Contribution of Working Group I to the Sixth Assessment Report of the Intergovernmental Panel on Climate Change* (eds Masson-Delmotte, V. et al.), pp. 1513–1766 (Cambridge Univ. Press, 2021).
9. Mandel, J. et al. Recent advances and applications of WRF–SFIRE. *Nat. Hazards Earth Syst. Sci.* **14**, 2829–2845 (2014).
10. Rabin, S. S. et al. The Fire Modeling Intercomparison Project (FireMIP), phase 1: experimental and analytical protocols with detailed model descriptions. *Geosci. Model Dev.* **10**, 1175–1197 (2017).
11. Goss, M. et al. Climate change is increasing the likelihood of extreme autumn wildfire conditions across California. *Environ. Res. Lett.* **15**, 094016 (2020).
12. Williams, A. P. et al. Observed impacts of Anthropogenic climate change on wildfire in California. *Earths Future* **7**, 892–910 (2019).
13. Abatzoglou, J. T. & Williams, A. P. Impact of anthropogenic climate change on wildfire across western US forests. *Proc. Natl Acad. Sci. USA* **113**, 11770–11775 (2016).
14. Seager, R. et al. Climatology, variability, and trends in the U.S. vapor pressure deficit, an important fire-related meteorological quantity. *J. Appl. Meteorol. Climatol.* **54**, 1121–1141 (2015).
15. Jolly, W. M. et al. Climate-induced variations in global wildfire danger from 1979 to 2013. *Nat. Commun.* **6**, 7537 (2015).
16. van Oldenborgh, G. J. et al. Attribution of the Australian bushfire risk to anthropogenic climate change. *Nat. Hazards Earth Syst. Sci.* **21**, 941–960 (2021).
17. Abatzoglou, J. T., Williams, A. P. & Barbero, R. Global emergence of Anthropogenic climate change in fire weather indices. *Geophys. Res. Lett.* **46**, 326–336 (2019).
18. Jain, P., Castellanos-Acuna, D., Coogan, S. C. P., Abatzoglou, J. T. & Flannigan, M. D. Observed increases in extreme fire weather driven by atmospheric humidity and temperature. *Nat. Clim. Change* **12**, 63–70 (2022).
19. Wang, S. S.-C., Qian, Y., Leung, L. R. & Zhang, Y. Identifying key drivers of wildfires in the contiguous US using machine learning and game theory interpretation. *Earths Future* **9**, e2020EF001910 (2021).
20. Huang, Y., Jin, Y., Schwartz, M. W. & Thorne, J. H. Intensified burn severity in California's northern coastal mountains by drier climatic condition. *Environ. Res. Lett.* **15**, 104033 (2020).
21. Elia, M. et al. Estimating the probability of wildfire occurrence in Mediterranean landscapes using Artificial Neural Networks. *Environ. Impact Assess. Rev.* **85**, 106474 (2020).
22. Satir, O., Berberoglu, S. & Donmez, C. Mapping regional forest fire probability using artificial neural network model in a Mediterranean forest ecosystem. *Geomat. Nat. Hazards Risk* **7**, 1645–1658 (2016).
23. Werth, P. A. et al. *Synthesis of Knowledge of Extreme Fire Behavior: Volume 2 for Fire Behavior Specialists, Researchers, and Meteorologists*. General Technical Report PNW-GTR-891 (U.S. Department of Agriculture, Forest Service, Pacific Northwest Research Station, 2016).
24. Schär, C., Frei, C., Lüthi, D. & Davies, H. C. Surrogate climate-change scenarios for regional climate models. *Geophys. Res. Lett.* **23**, 669–672 (1996).
25. Patricola, C. M. & Wehner, M. F. Anthropogenic influences on major tropical cyclone events. *Nature* **563**, 339–346 (2018).

26. Otto, F. E. L. Attribution of weather and climate events. *Annu. Rev. Environ. Resour.* **42**, 627–646 (2017).
27. French, N. H. F., Kasischke, E. S. & Williams, D. G. Variability in the emission of carbon-based trace gases from wildfire in the Alaskan boreal forest. *J. Geophys. Res.* **108**, FFR 7-1–FFR 7-11 (2003).
28. Flannigan, M. D., Logan, K. A., Amiro, B. D., Skinner, W. R. & Stocks, B. J. Future area burned in Canada. *Clim. Change* **72**, 1–16 (2005).
29. Conard, S. G. et al. Determining effects of area burned and fire severity on carbon cycling and emissions in Siberia. *Clim. Change* **55**, 197–211 (2002).
30. Potter, B. E. & McEvoy, D. Weather factors associated with extremely large fires and fire growth days. *Earth Interact.* **25**, 160–176 (2021).
31. Gutierrez, A. A. et al. Wildfire response to changing daily temperature extremes in California's Sierra Nevada. *Sci. Adv.* **7**, eabe6417 (2021).
32. Philip, S. et al. A protocol for probabilistic extreme event attribution analyses.*Adv. Stat. Climatol. Meteorol. Oceanogr.* **6**, 177–203 (2020).
33. Bindoff, N. L. et al. in *Climate Change 2013: The Physical Science Basis. Contribution of Working Group I to the Fifth Assessment Report of the Intergovernmental Panel on Climate Change* (ed. Stocker, T. F.), pp. 857–952 (Cambridge Univ. Press, 2013).
34. Duane, A., Castellnou, M. & Brotons, L. Towards a comprehensive look at global drivers of novel extreme wildfire events. *Clim. Change* **165**, 43 (2021).
35. Woollings, T. et al. Blocking and its response to climate change. *Current Clim. Change Rep.* **4**, 287–300 (2018).
36. Swain, D. L. A shorter, sharper rainy season amplifies California wildfire risk. *Geophys. Res. Lett.* **48**, e2021GL092843 (2021).
37. Zhuang, Y., Fu, R., Santer, B. D., Dickinson, R. E. & Hall, A. Quantifying contributions of natural variability and anthropogenic forcings on increased fire weather risk over the western United States. *Proc. Natl Acad. Sci.* **118**, e2111875118 (2021).
38. Stephens, S. L. et al. Drought, tree mortality, and wildfire in forests adapted to frequent fire. *BioScience* **68**, 77–88 (2018).
39. Westerling, A. L. Increasing western US forest wildfire activity: sensitivity to changes in the timing of spring. *Philos. Trans. R. Soc. B Biol. Sci.* **371**, 20150178 (2016).
40. Ma, W. et al. Assessing climate change impacts on live fuel moisture and wildfire risk using a hydrodynamic vegetation model. *Biogeosciences* **18**, 4005–4020 (2021).

Data availability

The Weather Research and Forecasting model used for the predictor data (Supplementary Information 3) is an open source and can be downloaded from GitHub (https://github.com/wrf-model/WRF/releases). MODIS fire products that were used for the predictand data (Supplementary Information 2) can be downloaded from FIRMS (https://firms.modaps.eosdis.nasa.gov/active_fire/) and the CMIP6 climate model data (Supplementary Information 4) can be downloaded from IPCC WGI Interactive Atlas (https://interactive-atlas.ipcc.ch/regional-information). Source data are provided with this paper.

Code availability

The code for this study is archived at GitHub (https://github.com/ptbrown31/Climate-Driven-Risk-of-Extreme-Wildfire-in-California).

Acknowledgements San José State's Wildfire Interdisciplinary Research Center (WIRC) is supported by the National Science Foundation (NSF)'s Industry–University Cooperative Research Center (IUCRC) Program (award number 2113931). We thank the Pacific Gas and Electric Meteorology Operations and Fire Science team for useful discussion throughout the project. We acknowledge the teams at DTN (https://www.dtn.com/), Atmospheric Data Solutions (http://www.atmosphericdatasolutions.com/) and Sonoma Technology (http://www.sonomatech.com/) for data collection and preprocessing. We also acknowledge M. Voss for technical support and A. J. Eiserloh, R. Bagley and P. Pall for valuable discussions. This project was partially funded by a contract (C6909) between the San José State University Research Foundation and Pacific Gas and Electric titled 'Understanding Extreme Fire Weather Conditions Using a 30-Year High-Resolution WRF Model Dataset'. A.M. was supported by the Director, Office of Science, Office of Biological and Environmental Research of the US Department of Energy as part of the Regional and Global Model Analysis program area within the Earth and Environmental Systems Modeling Program under contract number DE-AC02-05CH11231.

Author contributions S.J.S. introduced P.T.B. and H.H. to the broad conceptual framework used in this study (using machine learning models to predict the risk of extreme wildfire growth), and P.T.B. and H.H. worked together to refine the conceptual framework for climate-change-related applications. P.T.B. conceived of the specific methodology of the study, performed all the analyses and wrote an initial draft of the paper. A.M. and C.R. contributed to the technical and philosophical aspects of the machine learning experiment design and validation. S.J.D. created a schematic for Fig. 1 and helped refine communication (including figure design) throughout the study. A.K.K. and C.B.C. provided domain expertise in wildfire science, advising on which predictor variables to use. P.T.B., H.H., A.M., C.R., S.J.S., S.J.D., AKK. and C.B.C. all contributed to the interpretation of results and refinement of the manuscript.

Competing interests The authors declare no competing interests.

Additional information
Supplementary information The online version contains supplementary material available at https://doi.org/10.1038/s41586-023-06444-3.
Correspondence and requests for materials should be addressed to Patrick T. Brown.
Peer review information *Nature* thanks Mike Flannigan and the other, anonymous, reviewer(s) for their contribution to the peer review of this work. Peer reviewer reports are available.
Reprints and permissions information is available at http://www.nature.com/reprints.